Journal of Medicinal Chemistry

Article

pubs.acs.org/jmc

Antiproliferative and Antimigratory Actions of Synthetic Long Chain n-3 Monounsaturated Fatty Acids in Breast Cancer Cells That Overexpress Cyclooxygenase-2

Pei H. Cui,[†] Tristan Rawling,[†] Kirsi Bourget,[†] Terry Kim,[†] Colin C. Duke,[‡] Munikumar R. Doddareddy,[‡] David E. Hibbs,[‡] Fanfan Zhou,[†] Bruce N. Tattam,[§] Nenad Petrovic,[¶] and Michael Murray*[,†]

[†]Pharmacogenomics and Drug Development Group, [‡]Pharmaceutical Chemistry, and [§]Thomas R. Watson Mass Spectrometry Facility, Faculty of Pharmacy, University of Sydney, NSW 2006, Australia

[¶]Pharmacy and Medical Sciences, University of South Australia, GPO Box 2471, Adelaide SA 5001, Australia

Supporting Information

ABSTRACT: Cyclooxygenase-2 (COX-2) is overexpressed in many human cancers and converts the n-6 polyunsaturated fatty acid (PUFA) arachidonic acid to prostaglandin E_2 (PGE_2), which drives tumorigenesis; in contrast, n-3 PUFA inhibit tumorigenesis. We tested the hypothesis that these antitumor actions of n-3 PUFA may involve the n-3 olefinic bond. n-3 Monounsaturated fatty acids (MUFAs) of chain length C16−C22 were synthesized and evaluated in MDA-MB-468 breast cancer cells that stably overexpressed COX-2 (MDA-COX-2 cells). Longer chain (C19−C22) n-3 MUFAs inhibited proliferation, activated apoptosis, decreased PGE_2 formation, and decreased cell invasion; C16−C18 analogues were less active. Molecular modeling showed that interactions of Arg120, Tyr355, and several hydrophobic amino acid residues in the COX-2 active site with C19−C22 MUFA analogues were favored. Thus, longer-chain n-3 MUFAs may be prototypes of novel anticancer agents that decrease the formation of PGE_2 in tumor cells that contain high levels of COX-2.

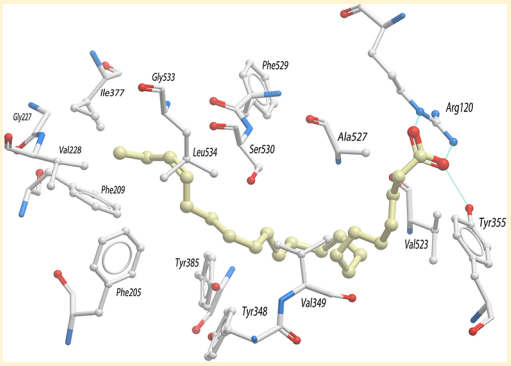

INTRODUCTION

The major cause of death from breast, prostate, and other cancers is metastatic disease in which cells migrate from the original tumor site to distant organs and establish secondary tumors.[1] Metastasis also frequently renders the tumor unresponsive to subsequent drug treatment and, because of their disseminated nature, surgical removal of metastases is not feasible.[2] The metastatic process is complex, involving the interplay of several discrete processes, including increased cell proliferation, invasion and angiogenesis.

n-3 and n-6 Polyunsaturated fatty acids (PUFAs) are two major classes of essential dietary fatty acids, exemplified by eicosapentaenoic acid (EPA; n-3, C20:5) and arachidonic acid (AA; n-6, C20:4), respectively. EPA and AA are structurally analogous, but EPA has an additional olefinic double bond at the n-3 position located between carbons 17 and 18. Numerous epidemiological studies in man and experimental studies in cells and animals have suggested that n-3 PUFAs like EPA offer potential benefits in cancer treatment by decreasing tumor growth and metastasis, whereas n-6 PUFAs are tumor-promoting. Thus, in a large cohort of French patients, increased content of n-3 docosahexaenoic or α-linolenic acids in breast adipose tissue is associated with improved survival compared with women in the lowest intake group.[3] In xenograft mouse models the spread of lung metastases produced by human breast cancer cells is decreased by EPA and docosahexaenoic acid.[4,5] Dietary PUFA are not only important risk factors for tumor progression but may also offer opportunities for the development of new cancer therapeutics.

n-3 and n-6 PUFAs are substrates for cyclooxygenase (COX), lipoxygenase, and cytochrome P450 enzymes and undergo biotransformation to parallel series of eicosanoid metabolites, including prostaglandins (PGs), leukotrienes, and epoxides. n-6-Derived PGs, especially PGE_2, are strongly implicated in tumor growth and metastasis.[6,7] There are two major COX genes in man: COX-1 is constitutively expressed in a wide range of tissues, while the constitutive expression of COX-2 is negligible but is strongly induced by proinflammatory cytokines and extracellular stress stimuli.[8,9] COX-2 is overexpressed to a much greater extent than COX-1 in many human breast and epithelial cell cancers and is associated with increased rates of PGE_2 production, which augments tumor progression and metastasis, leading to a poor prognosis.[7,8,10]

COX-2 inhibitors such as celecoxib have been shown to decrease mammary tumor burden in animal models by increasing tumor cell apoptosis, decreasing proliferation, and suppressing angiogenesis.[11−13] However, while nonsteroidal

Received: May 15, 2012
Published: July 23, 2012

Scheme 1. Synthesis of n-3 MUFAs[a]

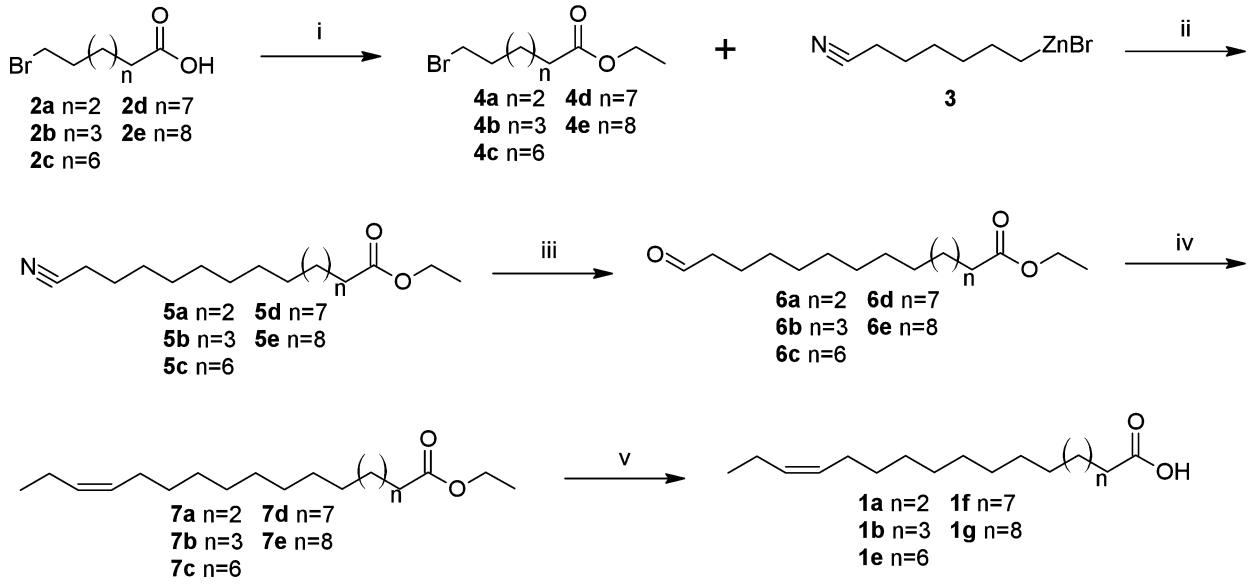

[a]Reagents and conditions: (i) Acetyl chloride, EtOH, rt, 4 h; (ii) PEPPSI-iPr, LiBr, THF/*N*-methyl-2-pyrrolidone (2:1), rt, 18 h; (iii) Raney Ni, NaH_2PO_2, pyridine/H_2O/AcOH (2:1:1), 40 °C, 2 h; (iv) $[Ph_3PPr]Br$, $NaN(TMS)_2$, −78 °C to rt, 2 h; (v) 1.5 M NaOH, ethanol, rt, 3 h.

anti-inflammatory drugs effectively inhibit tumorigenesis, the use of these agents in longer-term preventive treatment for cancer is impractical because of toxicity.[14] The identification of well-tolerated alternate agents that decrease PGE_2-dependent tumor cell migration by selective inhibition of COX-2 may assist the development of novel antimetastatic therapies. From studies in animals, the antimetastatic actions of n-3 PUFA are mediated in part by inhibiting COX-2 activity and PGE_2 formation.[5] Thus, increasing the dietary intake of n-3 PUFAs could be a viable strategy to impair PGE_2 production by tumors and improve health outcomes. However, because long-term patient compliance with altered dietary regimen is rarely successful, there is a need to develop effective new chemical entities. In the present study we synthesized a series of novel n-3 monounsaturated fatty acid (MUFA) derivatives based on naturally occurring n-3 PUFAs and evaluated their potential as inhibitors of breast cancer cell growth and migration. The principal finding to emerge was that the longer chain n-3 MUFA analogues (C20−C22) effectively decreased the growth and invasion capacity of breast cancer cells that overexpress COX-2 and markedly decreased PGE_2 production by these cells.

RESULTS

Synthesis of n-3 MUFA Analogues. We have previously described the facile synthesis of the C18 and C19 n-3 MUFA **1c** and **1d**.[15] The key C15 and C16 oxo-fatty acids (analogous to **6**, Scheme 1), that were used in Wittig reactions to construct the n-3 olefinic bonds in **1c** and **1d**, were obtained by esterification and subsequent oxidation of 15-hydroxypentadecanoic acid and 16-hydroxyhexadecanoic acid, respectively. However, because precursor ω-hydroxy-fatty acids required for synthesis of the analogues **1a**,**b**,**e**−**g** by that route are not commercially available, we developed a general strategy for the preparation of long chain oxo-fatty acids that utilized alkyl−alkyl Negishi cross-coupling reactions catalyzed by the N-heterocyclic carbene [1,3-bis(2,6-diisopropylphenyl)imidazol-2-ylidene](3-chloropyridyl)palladium(II) dichloride (PEPPSI-IPr;[16] Scheme 1). Prior to cross-coupling, carboxylic acid groups were protected by esterification with acetyl chloride and ethanol (Scheme 1). Subsequent alkyl−alkyl Negishi coupling of ethyl esters **4a**−**e** with the alkyl zinc reagent **3** proceeded in good yield (Scheme 1).[16] Selective reduction of the nitrile groups of **5a**−**e**, without concurrent reduction of the ester group, was achieved with Raney nickel/sodium hypophosphite,[17,18] affording the aldehyde intermediates **6a**−**e** in good yields (Scheme 1). The Wittig reaction, using THF as solvent and a coupling temperature of −78 °C, generated the n-3 bonds in **7a**−**e** with excellent (*Z*)-selectivities (*Z*:*E* ≥ 97:3). Double bond configurations and isomeric purities of **7a**−**e** were established using ^{13}C NMR and GC-MS due to overlapping olefinic proton resonances in the ^1H NMR spectra of **7a**−**e**.[15] Briefly, (*Z*)-geometries were confirmed from the chemical shifts of the resonances of carbon atoms that were adjacent to the olefinic bond. In n-3 double bonds these occur at ∼17 and 20 ppm and are diagnostic for the n-3 (*Z*)-configuration. Isomeric purity was accurately determined by GC-MS on a Zebron ZB-Wax column. Base-catalyzed hydrolysis of **7a**−**e** at room temperature then afforded the required n-3 MUFAs without the need for chromatography.

Antiproliferative and Apoptotic Actions of n-3 MUFA in Breast Cancer Cells. To evaluate the actions of the n-3 MUFAs against tumor cells in which COX-2 expression was high, we engineered the moderately invasive human breast cancer cell line MDA-MB-468 (MDA-CON) to overexpress COX-2 (MDA-COX-2 cells). As shown in Figure 1, basal expression of COX-2 immunoreactive protein in the parental cell line was low but was strongly expressed in the MDA-COX-2 stable transfectants. The effects of **1a**−**g** on the proliferation and viability of MDA-COX-2 cells were assessed by mitochondrial reduction of 3-(4,5-dimethylthiazol-2-yl)-2,5-diphenyltetrazolium bromide (MTT) and trypan blue exclusion. Basal mitochondrial MTT reduction measured after 48 h in culture was increased in MDA-COX-2 cells to 1.5 ± 0.1-fold of MDA-CON ($p < 0.01$), consistent with increased viability of the transfectants. Compounds **1a**−**g** elicited

dx.doi.org/10.1021/jm300673z | *J. Med. Chem.* 2012, 55, 7163−7172

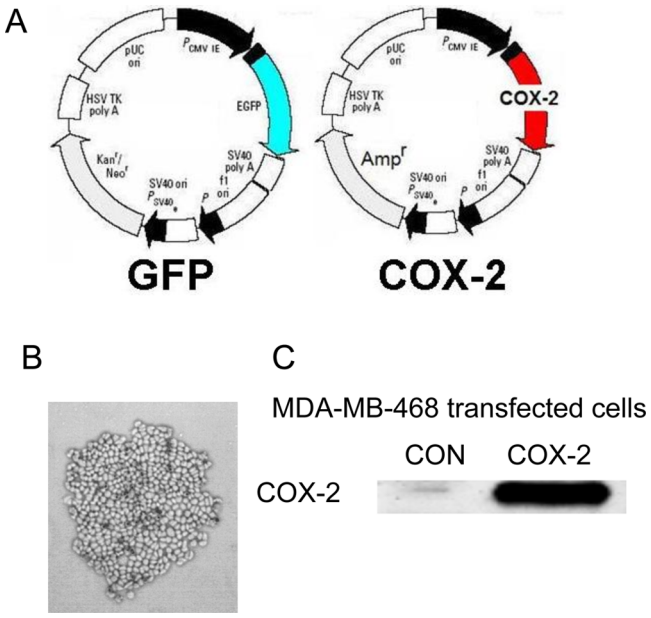

Figure 1. Construction of MDA-MB-468 cells that overexpressed COX-2 (MDA-COX-2 cells). (A) Plasmids encoding blank (GFP) and COX-2 used in transfections. (B) Colony formation in the presence of G418 antibiotic. (C) Immunoblot analysis of COX-2 protein expression in control (CON) and COX-2 cells.

concentration-related decreases in cell proliferation that were apparent after 24 h of treatment and IC_{50} values were determined after 48 h of treatment (Table 1). The C21 n-3 MUFA analogue (**1f**) exhibited the greatest antiproliferative potency (IC_{50} for inhibition of MTT reduction was 9.3 ± 2.9 μM), whereas the C22 (**1g**), C20 (**1e**), and C19 (**1d**) analogues were slightly less potent (IC_{50}s 21, 31, and 36 μM, respectively). In contrast, the short-chain analogues **1a**–**c** (C16–C18) were essentially inactive (IC_{50} >100 μM), while the naturally occurring n-3 and n-6 PUFAs EPA and AA also exhibited IC_{50}s that exceeded 100 μM.

Table 1. Antiproliferative and Proapoptotic Activities of n-3 MUFAs in MDA-COX-2 Breast Cancer Cells

analogue	carbon chain length	antiproliferative activity[a] (μM)	proapoptotic activity[b] (μM)
1a	16	>100	>100
1b	17	>100	69 ± 19
1c	18	>100	54 ± 12
1d	19	36 ± 4	43 ± 9
1e	20	31 ± 8	43 ± 0.2
1f	21	9.3 ± 2.9	12 ± 3
1g	22	21 ± 1	26 ± 5
AA	20	>100	>100
EPA	20	>100	>100

[a]MTT activity. [b]Caspase-3 activity.

To test whether the cytotoxic actions of the n-3 MUFAs were mediated by membrane disruption, MDA-COX-2 cells were treated with **1a**–**g** (20 and 50 μM) for 48 h, and viable cells were identified by trypan blue exclusion. However, only small decreases in viable cell number (by 25 ± 2% and 20 ± 2% from control) were apparent with the analogues **1a** (C16) and **1d** (C19), and only at the higher concentration; none of the other analogues induced membrane disruption.

The relationship between the growth inhibitory actions of the n-3 MUFAs and the activation of cellular apoptosis was assessed. Consistent with the observed decreases in cell proliferation the C21 analogue **1f** potently activated the key proapoptotic enzyme caspase-3 (EC_{50} 12 ± 3 μM; Table 1), while the C19, C20, and C22 analogues were somewhat less effective (EC_{50} range 26 to 43 μM); the shorter chain analogues (C16–C18), as well as the naturally occurring PUFAs EPA and AA, were less active.

Inhibition of COX-2-Dependent Cell Invasion and PGE_2 Formation by n-3 MUFAs. COX-2 overexpression is associated with an increase in tumor cell invasion. Using the Matrigel droplet assay developed in this laboratory,[19] basal invasion activity of MDA-COX-2 cells was markedly increased to 300 ± 15% of MDA-CON cells that expressed only low levels of COX-2 (57 ± 3 versus 19 ± 2 migrated cells/20 h, $p < 0.001$; Figure 2A). The migration of MDA-COX-2 cells was further increased when the media was supplemented with exogenous AA (20 μM; $p < 0.05$) but was decreased by EPA (20 μM; $p < 0.05$). We tested the capacity of the novel n-3 MUFA derivatives to inhibit the migration of MDA-COX-2 cells. The C22 n-3 MUFA **1g** (10 μM) effectively decreased cell invasion to 48 ± 4% of the uninhibited rate, while compounds **1e**–**g**, when tested at a concentration of 20 μM, inhibited invasion to 75 ± 8%, 59 ± 3%, and 48 ± 1% of control ($P < 0.001$); **1a**–**d** were inactive (Figure 2B).

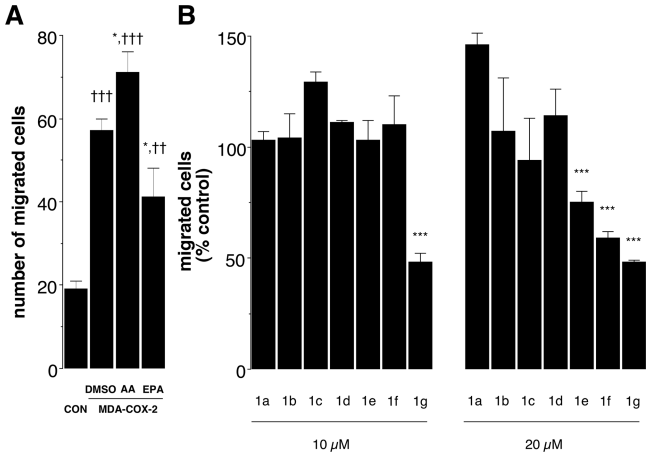

Figure 2. Effects of fatty acids on the number of cells that migrated in the Matrigel droplet assay over 20 h. (A) number of migrated MDA-COX-2 cells relative to MDA-MB-468 (CON) cells and effect of treatment with AA or EPA (20 μM) on migration. (B) Effect of treatment with n-3 MUFA (10 or 20 μM) on migration of MDA-COX-2 cells. Different from DMSO-treated MDA-COX-2 control: $^*p < 0.05$, $^{**}p < 0.01$, $^{***}p < 0.001$; different from MDA-CON cells: $^{\dagger\dagger}p < 0.01$, $^{\dagger\dagger\dagger}p < 0.001$.

PGE_2 is the most abundant eicosanoid that is generated by a range of tumors and has been shown to contribute significantly to cancer progression.[6,7,20,21] Basal secretion of PGE_2 into the media of cultured MDA-CON cells was undetectable by LC-MS-MS but was markedly increased in the medium from cultured MDA-COX-2 cells (68 ± 5 pmol/10^4 cells/48 h). In the present study, the effects of n-3 MUFAs (50 μM) on basal PGE_2 formation by MDA-COX-2 cells were investigated (Figure 3). Treatment with the longer chain n-3 MUFA **1e**–**g** (50 μM; 48 h) decreased basal PGE_2 formation to 46 ± 4%, 49 ± 8%, and 45 ± 4% of control, respectively, while

dx.doi.org/10.1021/jm300673z | J. Med. Chem. 2012, 55, 7163–7172

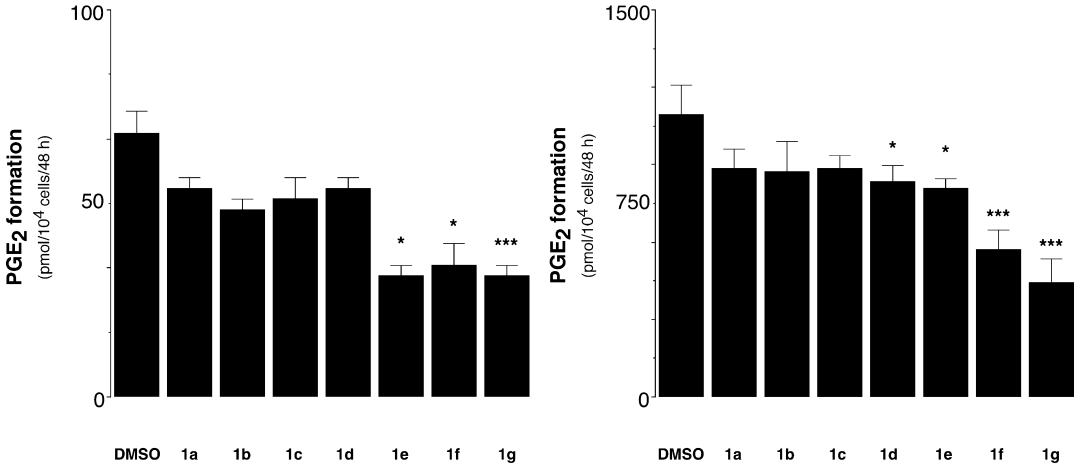

Figure 3. Effect of n-3 MUFAs (50 μM) on the secretion of PGE_2 into the media of MDA-COX-2 cells over 48 h in culture. (A, left) Basal PGE_2 secretion, and (B, right) AA-augmented PGE_2 secretion. Different from control: *$p < 0.05$, ***$p < 0.001$.

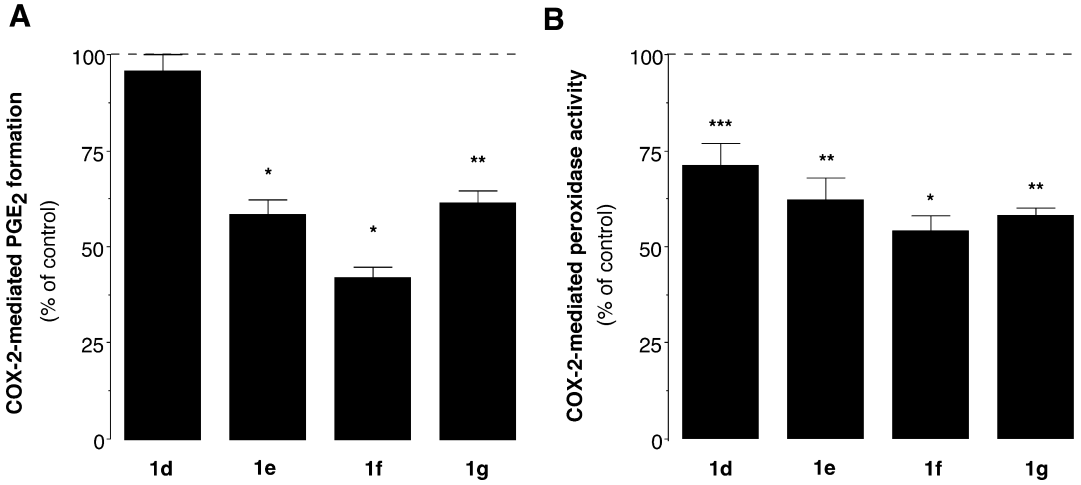

Figure 4. Inhibition of COX-2 activity in lysates of MDA-COX-2 cells by n-3 MUFA (50 μM). (A) Inhibition of PGE_2 formation, and (B) inhibition of peroxidase activity. Different from control: *$p < 0.05$, **$p < 0.01$, ***$p < 0.001$.

compounds **1a–d** were inactive. Co-incubation of MDA-COX-2 cells with AA (20 μM) enhanced PGE_2 formation to 16-fold of the basal rate (1.08 ± 0.12 nmol/10^4 cells/48 h; Figure 3B). The longer chain n-3 MUFAs (**1f**, **1g**) effectively decreased AA-augmented PGE_2 secretion to 40–52% of control (Figure 3B).

Because the longer chain n-3 MUFA inhibited the formation of PGE_2 by MDA-COX-2 cells we directly tested their capacity to inhibit COX-2 activity in cell lysates. These analogues decreased both basal and AA-supplemented PGE_2 formation in MDA-COX-2 breast cancer cells. In the presence of AA (20 μM), basal PGE_2 formation in lysates was 11.6 ± 3.1 fmol/mg protein/min that was readily suppressed by **1e–g** (50 μM) to 42–62% of AA-stimulated formation ($P < 0.01$); compound **1d** was less effective (Figure 4A). This finding was substantiated by testing the longer chain n-3 MUFA analogues against COX-2-mediated peroxidation of *N,N,N′,N′*-tetramethyl-*p*-phenylenediamine.[22] As anticipated, the activity was increased in MDA-COX-2 cell lysates to 2.3-fold of that in lysates from MDA-CON cells (24 ± 5 U/mL compared to 10 ± 2 U/mL). Compounds **1f** and **1g** (50 μM) decreased peroxidase activity to 54 ± 4% and 58 ± 2% of control, while **1d** and **1e** were somewhat less effective (71 ± 6% and 62 ± 6% decreases in activity; $P < 0.05$; Figure 4B). Together these findings are consistent with the capacity of the synthetic longer chain n-3 MUFAs to inhibit COX-2-dependent PGE_2 formation, which results in impaired cell viability, increased apoptosis and decreased invasion potential.

Modeling of n-3 MUFA in the Active Center of COX-2. To understand the interactions of the n-3 MUFAs with COX-2 in greater detail, compounds **1a–g** were docked into the active site of the enzyme (PDB code: 3HS5) (see Experimental Section for details of the computational modeling). As shown in Figure 5, the carboxylate groups of the n-3 MUFA analogues **1a** and **1g** are H-bonded to the Tyr355 (1.79 Å) and in a bifurcated manner to Arg120 (1.93, 1.92 Å). These are important residues in COX-2 that are adjacent to the entrance of the substrate access channel to the enzyme binding center and are involved in binding of PUFA substrates and COX inhibitors.[23,24] Additional stabilization of the binding of the longer chain analogue **1g** is provided by the extension of the ω-end of the molecule into a hydrophobic groove enclosed by the residues Phe205, Phe209, Gly227, Val228, Ile377, Gly533, and Leu534 and that is located above the catalytic Ser530 residue (Figure 5B). However, in the case of the shorter chain n-3 MUFAs, exemplified by the C16 analogue **1a**, extension into the hydrophobic groove was minimal, and bonding interactions with Tyr355 (2.58 Å) and Arg120 (1.96, 2.18 Å) are slightly weaker than for **1g** (Figure 5A). This decreased the number of

dx.doi.org/10.1021/jm300673z | J. Med. Chem. 2012, 55, 7163–7172

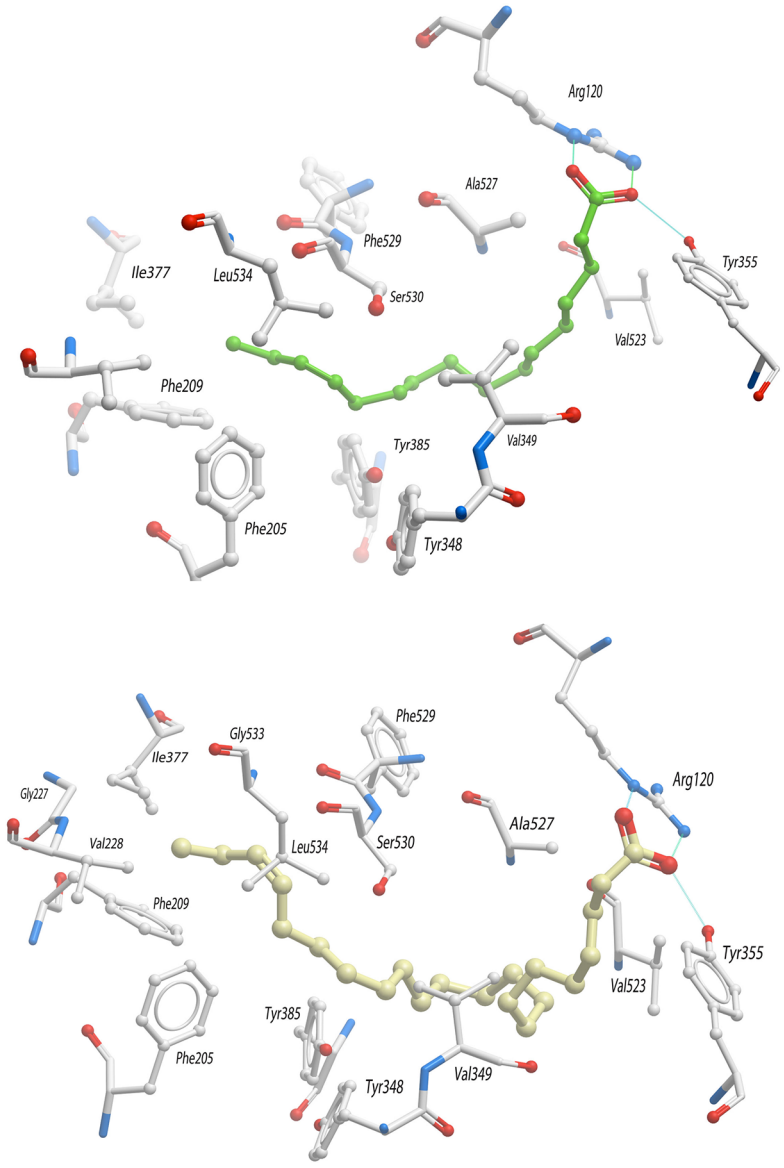

Figure 5. Docking of the n-3 MUFA analogues (A, upper) **1a** and (B, lower) **1g** into the COX-2 active site.

Table 2. Summary of XP[47] Docking Results and Prime MMGBSA ΔG Values[a]

compound	G_{Score}	Lipophilic EvdW	PhobEn	HBond	Electro	LowMW	RotPenal	LSE	$\Delta G_{bind\text{-}gs}$ [b]	$\Delta G_{bind\text{-}gbsa}$ [c]
1a	−10.11	−5.61	−2.51	−1.79	−0.51	−0.50	2.81	8.58	−7.53	−31.02
1b	−10.44	−5.88	−2.70	−1.65	−0.48	−0.50	2.78	7.10	−7.85	−40.61
1c	−11.11	−6.50	−2.70	−1.65	−0.50	−0.50	2.74	5.30	−8.44	−41.40
1d	−11.32	−6.29	−2.70	−1.98	−0.55	−0.50	2.70	6.59	−10.35	−46.88
1e	−13.12	−6.82	−2.70	−1.84	−0.62	−0.47	1.33	8.07	−10.55	−45.76
1f	−12.97	−6.90	−2.70	−1.74	−0.51	−0.42	1.30	7.85	−11.12	−45.00
1g	−13.48	−7.14	−2.70	−1.96	−0.58	−0.37	1.28	10.70	−11.33	−53.56

[a]Description of XP terms: G_{Score}: Total Glide Score; LipophilicEvdW: ChemScore lipophilic pair term and fraction of the total protein−ligand vdW energy; PhobEn: hydrophobic enclosure reward; HBond: ChemScore H-bond pair term; Electro: electrostatic rewards; LowMW: reward for ligands with low molecular weight; RotPenal: rotatable bond penalty; LSE: ligand strain energy in kcal/mol. [b]$\Delta G_{bind\text{-}gs}$ in kcal/mol calculated using Glide 'score in place' method. More details on scoring function employed can be found in the Supporting Information. [c]$\Delta G_{bind\text{-}gbsa}$ in kcal/mol calculated using Prime MMGBSA method. More details on scoring function employed can be found in the Supporting Information.

contacts made with the protein and the quality of the interaction (as reflected by the parameters derived using the Glide program; Table 2). Because the COX-2/MUFA interactions are principally hydrophobic in nature it would be anticipated that the van der Waals (vdW) contribution would strongly influence the overall binding energy. Thus, compared to shorter chain analogues, the longer carbon chains exhibited superior lipophilic character that improved vdW interactions (lipophilic EvdW) and negative effects on bond rotation (RotPenal) that were major components of G_{score} calculations.

dx.doi.org/10.1021/jm300673z | J. Med. Chem. 2012, 55, 7163−7172

Indeed, the G_{score} values for the longer chain analogues (**1e**−**g**) were higher (range −12.97 to −13.48) than those of shorter chain length (**1a**−**1d**) (range −10.11 to −11.32).

The calculation of absolute values for ΔG_{bind} is a challenging task in the absence of experimental values. Two methods are presented here: Glide's "score in place" method and Prime's molecular mechanics and surface-generalized Born solvation model (MM-GBSA). The ΔG_{bind} values obtained by using the (MM-GBSA) model gave values of $\Delta G_{bind\text{-}gbsa}$ that were unrealistically large, compared to those obtained from Glide ($\Delta G_{bind\text{-}gs}$), although they follow the same overall pattern, also favoring ligands with longer chain length. Thus, a $\Delta G_{bind\text{-}gbsa}$ value of −53.56 kcal/mol was calculated for **1g**, whereas the $\Delta G_{bind\text{-}gbsa}$ for the C16 analogue **1a** was only −31.02 kcal/mol (Table 2). $\Delta G_{bind\text{-}gs}$ gave in comparison, more typical values in the −7 to −11 kcal/mol range; these values again followed a similar trend to those obtained from the more rigorous MM-GBSA method (Table 2). G_{scores} and ΔG values were well correlated (r 0.81 and 0.93, for $\Delta G_{bind\text{-}gbsa}$ and $\Delta G_{bind\text{-}gs}$, respectively; Table 2).

The protein and MUFA strain energies are 20.56 and 8.58 kcal/mol, respectively, in the case of the interaction of **1g** with COX-2, whereas for **1a** there is a 10-fold increase in the protein strain energy (213.61 kcal/mol) and a more modest increase in MUFA strain (10.70 kcal/mol). Taken together, the parameters calculated from modeling studies are consistent with the experimentally observed inhibitory effects of the longer chain n-3 MUFAs on COX-2 activity and the diminished potencies of the short chain analogues.

DISCUSSION

COX-2 is overexpressed in ∼40% of human invasive breast cancers, and COX-2-derived PGE_2 is implicated in breast cancer metastasis.[10,12,25] In clinical studies, PGE_2 formation is associated with a high potential for metastasis by driving tumor proliferation and inhibiting apoptosis and results in adverse prognoses.[26] In mammary tissue of female COX-2-transgenic mice, several changes, including hyperplasia of terminal ductal lobules, epithelial neoplasia, and increased tumor cell invasive behavior, were noted that are consistent with accelerated tumorigenesis due to overproduction of PGE_2.[7] In vitro findings in cells are consistent with these observations. Thus, COX-2 overexpression promoted the growth and invasion potential of breast cancer cells[27,28] Overexpression of COX-2 enhanced the secretion of PGE_2 by tumor cells and activated angiogenesis in adjacent endothelial cells by augmenting the angiopoietin/vascular endothelial growth factor axis.[7,21] Considered together, inhibition of COX-2-derived PGE_2 formation may be a strategy that could be exploited to minimize tumor growth, metastasis, and angiogenesis.

Nonsteroidal anti-inflammatory drugs and COX-2-selective inhibitors have been found to inhibit tumor metastasis in vitro and in vivo.[7,29−32] Thus, celecoxib treatment inhibited COX-2 activity and PGE_2 secretion and arrested the growth of breast cancer cell lines.[20] In highly invasive MDA-MB-231 breast cancer cells, the mechanism of celecoxib-induced growth arrest involved induction of apoptosis, as reflected by caspase activation. In mouse orthotopic and xenograft models, the daily administration of celecoxib significantly decreased the growth and migration of tumor cells and activated apoptosis; tumor vascularization was also decreased.[12,13,33] Unfortunately, however, the toxicity of most nonsteroidal anti-inflammatory agents and COX-2-selective inhibitors precludes their long-term use as antimetastatic agents, and there is a need for alternative well-tolerated molecules that selectively inhibit COX-2-dependent formation of PGE_2 and minimize tumor spread.

n-3 PUFA, such as EPA, offer apparent benefits in the management of invasive cancers. Their antitumor actions have been attributed to decreased formation of COX-2-derived PGE_2.[34] However, the potencies of naturally occurring n-3 PUFA are limited by their intracellular availability, which would decline rapidly in cells because they undergo biotransformation by COX-2 and other enzymes. In addition, PUFAs have the potential for lipid peroxidation, which increases with the number of olefinic bonds but is minimized in saturated fatty acids.[35,36] To retain the antitumor actions of the n-3 olefinic bond without promoting lipid peroxidation, we prepared and evaluated a series of novel n-3 MUFA as potential anticancer agents. The longer chain n-3 MUFA analogues effectively inhibited the proliferation and invasion potential of breast cancer cells that were engineered to overexpress COX-2; these agents also activated apoptotic cell death. The potencies of the more active longer-chain n-3 MUFA analogues in the inhibition of proliferation and activation of apoptosis resembled those reported for clinically effective COX-2 inhibitors in cell-based assays. Thus, ibuprofen and naproxen directly inhibited wild-type COX-2 with IC_{50}s of 10 and 18 μM, respectively,[24] and a number of nonsteroidal anti-inflammatory agents inhibited the formation of PGE_2 in lipopolysaccharide-activated monocytes with IC_{50}s between 0.1 and 4 μM.[37]

Longer chain n-3 MUFAs effectively decreased COX-2-mediated PGE_2 formation and peroxidase activity in cells. When the n-3 MUFAs **1a**−**g** were docked into the active site of COX-2, they adopted an L-shaped configuration similar to those found with the naturally occurring n-6 PUFA AA and n-3 PUFA EPA.[38−40] The carboxylate groups in n-6 and n-3 PUFAs form an ion pair with Arg120 and a hydrogen bond with Tyr355 that are located at the entrance of the channel that controls the access of substrate to the active region of the enzyme. The ω-ends of the PUFA extend above Ser530 into an upper channel adjacent to Gly533 that is stabilized by Phe205, Phe209, Val228, and Leu534.[38] Binding is apparently stabilized by vdW interactions with methylene units in the aliphatic chain.[39] Thus, 54 and 56 contacts have been identified in modeling studies for interaction of AA and EPA, respectively, with residues that line the COX-2 active site. Similar to these findings, the aliphatic ω-ends of the n-3 MUFAs also extend into the hydrophobic groove that is adjacent to Ser530. The longer chain analogues (C20−C22) projected into the groove, whereas these contacts were minimal in the shorter chain analogues. In accord with these findings, Dong et al. found that MUFA analogues of short to intermediate chain length (C16−C20), that carried Δ^9 or Δ^{11} olefinic bonds, did not inhibit COX-2 activity, which suggests that they are unable to coordinate effectively into the substrate binding site of COX-2.[41]

Previous modeling studies with a range of clinically effective and experimental COX-2 inhibitors identified interactions with the active region of the enzyme that were similar to those of the present n-3 MUFA. Thus, from crystallography and molecular modeling, carboxylate substituents in these agents also interacted with Arg120 and Tyr355 and projected inward into hydrophobic clefts in the enzyme, which enabled interactions with hydrophobic amino acid residues that include Val349, Val523, Ala527, Ser530, and Leu534.[42,43] Together, the

findings from modeling studies account for the experimentally observed inhibitory effects of the longer chain n-3 MUFAs on COX-2 activity as well as the lower potencies of the shorter chain analogues. The present molecules emerge as prototypes of a novel class of anticancer agents that modulate cell metastasis; further structural modification may produce analogues with enhanced potency and efficacy in vivo.

EXPERIMENTAL SECTION

General Chemistry. All chemicals, including **4a**,**b**, and anhydrous solvents were purchased from Sigma Aldrich (Castle Hill, NSW, Australia). 9-Bromononanoic acid was prepared by the method of Duffy et al.[44] Dry column vacuum chromatography (DCVC) was used to purify reaction products on silica gel with gradient elution by hexane and dichloromethane. TLC was performed on silica gel 60 F_{254} plates, and products were visualized with ceric ammonium molybdate. The 400 MHz ^{1}H NMR and ^{13}C NMR spectra were recorded using a Varian 400-MR instrument and were referenced internally to $CDCl_3$ (^{1}H δ 7.26, ^{13}C δ 77.10). Melting points were measured on a Stuart SMP10 melting point apparatus. GC-MS was performed on a PolarisQ GC-MS-MS ion trap mass spectrometer coupled to a Trace GC, as described elsewhere.[15] Elemental analysis (C, H, N) was carried out by the Microanalytical Unit at the Research School of Chemistry, Australian National University (ACT, Australia), and all values were within ±0.4% of the calculated values.

General Method for Preparation of Bromo Ethyl Esters 4c–e: Ethyl 10-Bromodecanoate (4c). A solution of 10-bromodecanoic acid (2.500 g, 9.95 mmol) and acetyl chloride (3.907 g, 49.77 mmol) in ethanol (150 mL) was stirred at room temperature for 4 h. The solvent was removed in vacuo, and the residue was dissolved in diethyl ether (100 mL) and washed with saturated $NaHCO_3$ (2 × 70 mL), water (70 mL), and brine (70 mL). The organic phase was dried with Na_2SO_4, and concentrated in vacuo. The crude product was purified by silica gel DCVC, affording **4c** (2.456 g, 88%) as a colorless oil. The ^{1}H NMR and MS spectra of the product are in agreement with partial data previously reported.[45] ^{1}H NMR (400 MHz, $CDCl_3$): δ 4.11 (q, J_{HH} = 7.2 Hz, 2H), 3.39 (t, J_{HH} = 6.8 Hz, 2H), 2.27 (t, J_{HH} = 7.6 Hz, 2H), 1.84 (p, J_{HH} = 7.2 Hz, 2H), 1.61 (p, J_{HH} = 7.6 Hz, 2H), 1.41 (m, 2H), 1.28 (m, 8H), 1.24 (t, J_{HH} = 7.2 Hz, 3H). ^{13}C NMR (100 MHz, $CDCl_3$): δ 173.86, 60.14, 34.35, 34.01, 32.78, 29.21, 29.12, 29.06, 28.67, 28.11, 24.92, 14.25. CI-MS: m/z (%): 281 ([M + H]$^+$).

General Method for Preparation of Cyano Ethyl Esters 5a–e: Ethyl 12-Cyanododecanote (5a). Anhydrous LiBr (2.084 g, 24.00 mmol) and PEPPSI-IPr (0.096 g, 0.14 mmol) were dissolved in anhydrous THF (5 mL) and *N*-methyl-2-pyrrolidone (10 mL) under nitrogen. **4a** (1.575 g, 7.06 mmol) and then 6-cyanohexylzinc bromide solution (24 mL, 12 mmol) were added, and the solution was stirred at room temperature for 18 h. Diethyl ether (70 mL) was added, and the organic phase was washed with 1 M Na_3EDTA solution (50 mL), water (50 mL), and brine (50 mL). After drying with Na_2SO_4, the solvent was removed in vacuo, and the residue was purified on silica gel DCVC, affording **5a** (1.037 g, 58%) as a colorless oil. The ^{1}H and ^{13}C NMR spectra of the product are in good agreement with previously reported data.[46] CI-MS: m/z (%): 254 ([M + H]$^+$).

General Method for Preparation of Oxo Ethyl Esters 6a–e: Ethyl 13-Oxotridecanoate (6a). To a solution of **5a** (0.600 g, 2.37 mmol) in pyridine (20 mL) were added water (10 mL), acetic acid (10 mL), sodium hypophosphite (2.007 g, 18.93 mmol), and Raney nickel. The suspension was then stirred at 40 °C for 2 h. The catalyst was removed by filtration and washed with ethanol (2 mL). Water (150 mL) and diethyl ether (40 mL) were added to the filtrate, and the organic layer was separated. The aqueous phase was further extracted with diethyl ether (2 × 40 mL), and the combined extracts were washed with water (150 mL) and brine (80 mL). The extracts were concentrated in vacuo, and the residue was purified by silica gel DCVC, affording **6a** (0.432 g, 71%) as a colorless oil. ^{1}H NMR (400 MHz, $CDCl_3$): 9.76 (t, J_{HH} = 1.6 Hz, 1H), 4.11 (q, J_{HH} = 7.2 Hz, 2H), 2.41 (td, J_{HH} = 7.2, 1.6 Hz, 2H), 2.28 (t, J_{HH} = 7.6 Hz, 2H), 1.67–1.36 (m, 4H), 1.36–1.22 (m, 17H). ^{13}C NMR (100 MHz, $CDCl_3$): δ 202.98, 173.94, 60.16, 43.92, 34.39, 29.48, 29.40, 29.38, 29.34, 29.24, 29.16, 29.13, 24.98, 22.08, 14.26. CI-MS: m/z (%): 257 ([M + H]$^+$).

General Method for Preparation of n-3 MUFA Ethyl Esters 7a–e: Ethyl *cis*-13-Hexadecenoate (7a). To a suspension of *n*-propyltriphenylphosphonium bromide (0.885 g, 2.03 mmol) in anhydrous THF (4 mL) at 0 °C under a nitrogen atmosphere was added 1 M $NaN(TMS)_2$ (2.09 mL, 2.09 mmol). The resulting orange mixture was stirred for 40 min at room temperature and cooled to −78 °C, and **6a** (0.270 g, 1.04 mmol) in THF (3 mL) was added dropwise by syringe. Stirring at −78 °C was continued for 30 min after which the reaction mixture was warmed to room temperature. After further stirring for 1.5 h, the reaction was quenched with saturated NH_4Cl (20 mL) and extracted with dichloromethane (3 × 40 mL). The combined extracts were dried over Na_2SO_4 and concentrated in vacuo. The residue was purified by silica gel DCVC, affording **7a** (0.244 g, 83%) as a colorless oil. ^{1}H NMR (400 MHz, $CDCl_3$): 5.40–5.28 (m, 2H), 4.11 (q, J_{HH} = 7.2 Hz, 2H), 2.28 (t, J_{HH} = 7.2 Hz, 2H), 2.07–1.97 (m, 4H), 1.61 (quin, J_{HH} = 7.2 Hz, 2H), 1.37–1.20 (m, 19H), 0.95 (t, J_{HH} = 7.6 Hz, 3H). ^{13}C NMR (100 MHz, $CDCl_3$): δ 173.91, 131.49, 129.33, 60.12, 34.39, 29.76, 29.59, 29.56, 29.52, 29.44, 29.27, 29.25, 29.14, 27.08, 24.98, 20.49, 14.38, 14.24. CI-MS: m/z (%): 283 ([M + H]$^+$). t_R = 24.14 min. *Z*:*E* ratio = 98.0: 2.0.

General Method for Preparation of n-3 MUFAs 1a,b,e–g: *cis*-13-Hexadecenoic Acid (1a). To a solution of **7a** (0.099 g, 0.35 mmol) in ethanol (15 mL) was added 1.5 M NaOH (7.5 mL). The suspension was stirred at 45 °C until a solution was obtained. After the solution was stirred at room temperature for 3 h, the ethanol was removed in vacuo, and water (10 mL) was added. The mixture was adjusted to pH 2 with 1 M HCl, and the product was extracted with dichloromethane (3 × 20 mL), dried over Na_2SO_4, and concentrated in vacuo to afford **1a** as a white solid, mp 27–29 °C. ^{1}H NMR (400 MHz, $CDCl_3$): 5.40–5.23 (m, 2H), 2.35 (t, J_{HH} = 7.2 Hz, 2H), 2.07–1.98 (m, 4H), 1.63 (quin, J_{HH} = 7.6 Hz, 2H), 1.40–1.20 (m, 16H), 0.95 (t, J_{HH} = 7.2 Hz, 3H). ^{13}C NMR (100 MHz, $CDCl_3$): δ 179.06, 131.52, 129.36, 33.88, 29.78, 29.60, 29.57, 29.53, 29.43, 29.29, 29.24, 29.06, 27.10, 24.69, 20.51, 14.41. CI-MS (FAME): m/z (%): 269 ([M + H]$^+$). R_t (FAME) = 22.27 min. *Z*:*E* ratio =98.0: 2.0. Anal. Calcd for $C_{16}H_{30}O_2$: C 75.54, H 11.89. Found: C 75.84, H 11.69.

Cell Culture. Human MDA-MB-468 breast cancer cells were obtained from ATCC (Manassas, VA). COX-2 and green fluorescent protein expression plasmids (OriGene, Rockville, MD, and pEGFP-N1, Invitrogen, Mulgrave, VIC, Australia, respectively) under the control of the CMV promoter were transfected into MDA-MB-468 cells using Lipofectamine 2000. Media containing increasing concentrations of G418 (100–400 μg/mL) was used to select for stable transfectants, with resistance conferred by the plasmid-encoding green fluorescent protein. Positive clones were selected by G418 resistance, fluorescence microscopy, and immunoblotting for COX-2.

Cells were cultured in Dulbecco's Modified Eagle Medium supplemented with 10% fetal bovine serum (Thermo Fischer Scientific, Waltham, MA) and 1% penicillin/streptomycin (Invitrogen), and grown at 37 °C in a humidified atmosphere of 5% CO_2 in air. Confluent cells (80–90%) were harvested using trypsin/EDTA after washing in phosphate-buffered saline (Amresco, Solon, OH). Test compounds were dissolved in DMSO (Sigma-Aldrich)/2-propanol (Merck; Kilsyth, VIC, Australia) (final concentration 0.1%).

Cell Viability and Apoptosis. For MTT and caspase-3 activity assays, cells were seeded in 96-well plates at a density of 1 × 10^4 cells/mL. Cells were treated with MUFAs (0.1–200 μM) for 48 h with a change of media at 24 h. MTT activity was determined spectrophotometrically. IC_{50} values were determined from plots of "percent remaining MTT activity" versus "log [n-3 MUFA]." Caspase-3 activity was measured in cell lysates by luminometry (Caspase-Glo 3/7 kit, Promega; Alexandria, NSW, Australia). EC_{50} values were determined from plots of "percent caspase-3 activation" versus "log [n-3 MUFA]."

Matrigel Droplet Cell Migration Assay. Cells (3.5 × 10^6 cells/mL) were mixed with matrigel (Trevigen; Gaithersburg, MD), and 20 μL was loaded carefully onto the surface of six-well plates (Nunc; Roskilde, Denmark) to produce well-defined droplets. Plates were incubated for 5 min at 37 °C under 5% CO_2 to enable the matrigel

dx.doi.org/10.1021/jm300673z | J. Med. Chem. 2012, 55, 7163–7172

droplets to semisolidify.[19] Endothelial cell growth medium-2 that was supplemented with Single Quote and 10% fetal bovine serum (Cambrex Bioscience; Mt Waverley, VIC, Australia) was added to plates and incubated for 20 h under a 5% CO_2 atomosphere at 37 °C, after which cells that migrated out of matrigel droplets were counted by inverted phase-contrast microscopy (Olympus CKX41).

COX-2 Activity of Cell Lysates. The effects of n-3 MUFAs on COX-2 activity in confluent MDA-COX-2 cells (1×10^8) were determined by two approaches. Heme (10 μM), arachidonic acid (20 μM), and the n-3 MUFA analogues (50 μM) were incubated for 5 min at 25 °C in Tris-HCl buffer (100 mM, pH 8.0). COX-2-dependent peroxidase activity was measured spectrophotometrically at 590 nm by the oxidation of *N*,*N*,*N*′,*N*′-tetramethyl-*p*-phenylenediamine.[22] COX-2-dependent PGE_2 formation in cell lysates was determined similarly, except that quantification was by LC-MS-MS. After a 10 min incubation at 37 °C, ice-cold acetonitrile (0.8 mL) and internal standard PGE_2-d_4 (50 ng) were added and the mixture was loaded onto Oasis HLB SPE cartridges (Waters, Rydalmere, NSW, Australia). Eicosanoids were eluted with acetonitrile (4 mL) and ethyl acetate (2 mL), dried under nitrogen, and reconstituted in acetonitrile (100 μL) for LC-MS analysis.

Quantification of PGE_2 Formation. LC-MS-MS was performed on a Thermo Scientific TSQ Quantum Access Max System (Waltham, MA). Eicosanoids were separated using a Gemini-NX C_{18} 110A 3 μm 150 × 4.6 mm LC column (Phenomenex, Torrance, CA). Gradient elution was with acetonitrile:water:acetic acid (A: 15:85:0.02, B: 90:10:0.02) at an initial ratio of 65% A:35% B for 15 min, increasing to 35% A:65% B for 10 min, and then followed by a linear gradient from 35% A:65% B to 10% A:90% B over 10 min. The flow rate was 0.4 mL/min, the sample injection volume was 10 μL, and the MS was operated in the electrospray negative ion mode with nitrogen as the cone gas. The temperatures of the heated capillary and the vaporizer were 261 °C and 475 °C, respectively. The scan time was 2 s, and the interscan delay was 0.1 s. All eicosanoids were detected according to parent and fragmentation ions using Thermo Xcalibur 2.1 software (Thermo Fischer Scientific Inc., Waltham, MA).

Computational Modeling. MUFA structures were built, manipulated and adjusted for chemical correctness using Maestro (v9.1, Schrödinger, LLC, New York, NY) graphical user interface employing MacroModel (v9.1, Schrödinger, LLC). Geometry minimizations were performed on all ligands using the OPLS_2005 (MacroModel, v9.1, Schrödinger, LLC) force field and the Truncated Newton Conjugate Gradient. Optimizations were converged to a gradient rmsd below 0.012 kJ/mol or continued to a maximum of 500 iterations, at which point there were negligible changes in rmsd gradients.

MUFAs were independently docked into COX-2 with Glide (version 5.7, Schrödinger, LLC) utilizing the extra precision (XP) scoring function to estimate protein−MUFA binding affinities. The site targeted in the docking calculations was defined by the position of the AA molecule observed in complex with COX-2 as part of the crystal structure (PDB code: 3HS5). Protein preparation and refinement protocols directed by the protein preparation facility (Glide v5.7 Schrödinger, LLC) were performed on both target and molecule to achieve chemical correctness. Briefly, this included deleting crystallographic waters, adding hydrogens, adjusting bond orders and formal charges, and alleviating potential steric clashes via protein minimization with the OPLS_2005 force field. The shape and properties of the binding site were characterized and setup for docking using the receptor grid generation panel (Glide v5.7 Schrödinger, LLC). A Coulomb-vdW scaling of 1.0/0.8 was set for protein/MUFA vdW radii, respectively.

The induced-fit docking protocol was run from the graphical user interface accessible within Maestro 9.1. The overall procedure has four stages. Briefly, during stage 1, initial softened-potential Glide docking was performed on a vdW scaled-down rigid-protein; a scaling of 0.7/0.5 was set for protein/MUFA vdW radii, respectively. In stage 2, sampling and refinement were performed on residues within 5.0 Å of docked MUFA for each of the seven MUFA:protein complexes. Amino acid side chains, as well as the protein backbone and MUFA, underwent subsequent energy minimizations. A total of ten induced-fit protein conformations were generated for each of the test ligands. Stage 3 involved redocking the test molecules into the corresponding structures that were within 30.0 kcal/mol of the lowest energy structure. Finally, the ligand poses were scored in stage 4 using a combination of Prime and GlideScore scoring functions in which the top ranked pose for each MUFA was chosen as the final result. The XP scoring function was used in all docking stages.[47]

Statistical Analysis. All measurements were performed at least in duplicate with experiments replicated on at least three occasions. Data are presented throughout as mean ± SE and were analyzed by one-way ANOVA in combination with Fisher's Protected Least Significant Difference test to detect differences between multiple treatments.

■ ASSOCIATED CONTENT

Ⓢ Supporting Information

Analytical and spectroscopic data for all compounds, and G_{score} and ΔG_{bind} calculations. This material is available free of charge via the Internet at http://pubs.acs.org.

■ AUTHOR INFORMATION

Corresponding Author

*Tel: 61-2-9351-2326. Fax: 61-2-9351-4391. E-mail: michael.murray@sydney.edu.au.

Notes

The authors declare no competing financial interest.

■ ACKNOWLEDGMENTS

This study was supported by a grant from the Australian National Health and Medical Research Council.

■ ABBREVIATIONS USED

PUFA, polyunsaturated fatty acid; EPA, eicosapentaenoic acid; AA, arachidonic acid; COX, cyclooxygenase; PG, prostaglandin; MUFA, monounsaturated fatty acid; PEPPSI-IPr, [1,3-bis(2,6-diisopropylphenyl)imidazol-2-ylidene](3-chloropyridyl)-palladium(II) dichloride; MDA-CON, MDA-MB-468-control cells; MDA-COX-2, MDA-MB-468 cell-stable transfectants that overexpress COX-2; MTT, 3-(4,5-dimethylthiazol-2-yl)-2,5-diphenyltetrazolium bromide; MM-GBSA, molecular mechanics and surface-generalized Born solvation models; vdW, van der Waals; DCVC, dry column vacuum chromatography; XP, extra precision

■ REFERENCES

(1) Mehlen, P.; Puisieux, A. Metastasis: a question of life or death. *Nat. Rev. Cancer* **2006**, *6*, 449−458.

(2) Borst, P.; Jonkers, J.; Rottenberg, S. What makes tumors multidrug resistant? *Cell Cycle* **2007**, *6*, 2782−2787.

(3) Maillard, V.; Bougnoux, P.; Ferrari, P.; Jourdan, M. L.; Pinault, M.; Lavillonniere, F.; Body, G.; Le Floch, O; Chajes, V. N-3 and N-6 fatty acids in breast adipose tissue and relative risk of breast cancer in a case-control study in Tours, France. *Int. J. Cancer* **2002**, *98*, 78−83.

(4) Rose, D. P.; Connolly, J. M.; Rayburn, J.; Coleman, M. Influence of diets containing eicosapentaenoic or docosahexaenoic acid on growth and metastasis of breast cancer cells in nude mice. *J. Natl. Cancer Inst.* **1995**, *87*, 587−592.

(5) Rose, D. P.; Connolly, J. M.; Coleman, M. Effect of omega-3 fatty acids on the progression of metastases after the surgical excision of human breast cancer cell solid tumors growing in nude mice. *Clin. Cancer Res.* **1996**, *2*, 1751−1756.

(6) Schrey, M. P.; Patel, K. V. Prostaglandin E_2 production and metabolism in human breast cancer cells and breast fibroblasts. Regulation by inflammatory mediators. *Br. J. Cancer* **1995**, *72*, 1412−1419.

(7) Chang, S. H.; Liu, C. H.; Conway, R.; Han, D. K.; Nithipatikom, K.; Trifan, O. C.; Lane, T. F.; Hla, T. Role of prostaglandin E_2-dependent angiogenic switch in cyclooxygenase 2-induced breast cancer progression. *Proc. Natl. Acad. Sci. U.S.A.* **2004**, *101*, 591−596.
(8) Hwang, D.; Scollard, D.; Byrne, J.; Levine, E. Expression of cyclooxygenase-1 and cyclooxygenase-2 in human breast cancer. *J. Natl. Cancer Inst.* **1998**, *90*, 455−460.
(9) Hla, T.; Bishop-Bailey, D.; Liu, C. H.; Schaefers, H.; Trifan, O. C. Cyclooxygenase-1 and -2 isoenzymes. *Int. J. Biochem. Cell Biol.* **1999**, *31*, 551−557.
(10) Half, E.; Tang, X. M.; Gwyn, K.; Sahin, A.; Wathen, K.; Sinicrope, F. A. Cyclooxygenase-2 expression in human breast cancers and adjacent ductal carcinoma *in situ*. *Cancer Res.* **2002**, *62*, 1676−1681.
(11) Rozic, J. G.; Chakraborty, C.; Lala, P. K. Cyclooxygenase inhibitors retard murine mammary tumor progression by reducing tumor cell migration, invasiveness and angiogenesis. *Int. J. Cancer* **2001**, *93*, 497−506.
(12) Basu, G. D.; Pathangey, L. B.; Tinder, T. L.; Lagioia, M.; Gendler, S. J.; Mukherjee, P. Cyclooxygenase-2 inhibitor induces apoptosis in breast cancer cells in an *in vivo* model of spontaneous metastatic breast cancer. *Mol. Cancer Res.* **2004**, *2*, 632−642.
(13) Connolly, E. M.; Harmey, J. H.; O'Grady, T.; Foley, D.; Roche-Nagle, G.; Kay, E.; Bouchier-Hayes, D. J. Cyclo-oxygenase inhibition reduces tumor growth and metastasis in an orthotopic model of breast cancer. *Br. J. Cancer* **2002**, *87*, 231−237.
(14) Rao, C. V.; Reddy, B. S. NSAIDs and chemoprevention. *Curr. Cancer Drug Targets* **2004**, *4*, 29−42.
(15) Rawling, T.; Duke, C. C.; Cui, P. H.; Murray, M. Facile and stereoselective synthesis of (Z)-15-octadecenoic acid and (Z)-16-nonadecenoic acid: monounsaturated omega-3 fatty acids. *Lipids* **2010**, *45*, 159−165.
(16) Organ, M. G.; Avola, S.; Dubovyk, I.; Hadei, N.; Kantchev, E. A.; O'Brien, C. J.; Valente, C. A user-friendly, all-purpose Pd-NHC-(NHC=N-heterocyclic carbene) precatalyst for the Negishi reaction: a step towards a universal cross-coupling catalyst. *Chem.—Eur. J.* **2006**, *12*, 4749−4755.
(17) Backeberg, O. G.; Staskun, B. A novel reduction of nitriles to aldehydes. *J. Chem. Soc.* **1962**, 3961−3963.
(18) Heffner, R. J.; Jiang, J.; Joullie, M. M. Total synthesis of (−)-nummularine F. *J. Am. Chem. Soc.* **1992**, *114*, 10181−10189.
(19) Szymczak, M.; Murray, M.; Petrovic, N. Modulation of angiogenesis by ω-3 polyunsaturated fatty acids is mediated by cyclooxygenases. *Blood* **2008**, *111*, 3514−3521.
(20) Horia, E.; Watkins, B. A. Comparison of stearidonic acid and α-linolenic acid on PGE_2 production and COX-2 protein levels in MDA-MB-231 breast cancer cell cultures. *J. Nutr. Biochem.* **2005**, *16*, 184−192.
(21) Wang, D.; DuBois, R. N. Cyclooxygenase 2-derived prostaglandin E_2 regulates the angiogenic switch. *Proc. Natl. Acad. Sci. U.S.A.* **2004**, *101*, 415−416.
(22) Petrovic, N.; Murray, M. Using N,N,N′,N′-tetramethyl-p-phenylenediamine (TMPD) to assay cyclooxygenase activity *in vitro*. *Methods Mol. Biol.* **2010**, *594*, 129−140.
(23) Bhattacharyya, D. K.; Lecomte, M.; Rieke, C. J.; Garavito, M.; Smith, W. L. Involvement of arginine 120, glutamate 524, and tyrosine 355 in the binding of arachidonate and 2-phenylpropionic acid inhibitors to the cyclooxygenase active site of ovine prostaglandin endoperoxide H synthase-1. *J. Biol. Chem.* **1996**, *271*, 2179−2184.
(24) Rowlinson, S. W.; Kiefer, J. R.; Prusakiewicz, J. J.; Pawlitz, J. L.; Kozak, K. R.; Kalgutkar, A. S.; Stallings, W. C.; Kurumbail, R. G.; Marnett, L. J. A novel mechanism of cyclooxygenase-2 inhibition involving interactions with Ser-530 and Tyr-385. *J. Biol. Chem.* **2003**, *278*, 45763−45769.
(25) Ristimäki, A.; Sivula, A.; Lundin, J.; Lundin, M.; Salminen, T.; Haglund, C.; Joensuu, H.; Isola, J. Prognostic significance of elevated cyclooxygenase-2 expression in breast cancer. *Cancer Res.* **2002**, *62*, 632−635.
(26) Subbaramaiah, K.; Norton, L.; Gerald, W.; Dannenberg, A. J. Cyclooxygenase-2 is overexpressed in HER-2/neu-positive breast cancer: evidence for involvement of AP-1 and PEA3. *J. Biol. Chem.* **2002**, *277*, 18649−18657.
(27) Liu, X. H.; Rose, D. P. Differential expression and regulation of cyclooxygenase-1 and -2 in two human breast cancer cell lines. *Cancer Res.* **1996**, *56*, 5125−5127.
(28) Takahashi, Y. K. F.; Noguchi, M.; Miwa, K.; Sato, H.; Seiki, M.; Inoue, H.; Tanabe, T.; Yoshimoto, T. Activation of matrix metalloproteinase-2 in human breast cancer cells overexpressing cyclooxygenase-1 or -2. *FEBS Lett.* **1999**, *460*, 145−148.
(29) Sharpe, C. R.; Collet, J. P.; McNutt, M.; Belzile, E.; Boivin, J. F.; Hanley, J. A. Nested case-control study of the effects of non-steroidal anti-inflammatory drugs on breast cancer risk and stage. *Br. J. Cancer* **2000**, *83*, 112−120.
(30) Davies, G.; Salter, J.; Hills, M.; Martin, L. A.; Sacks, N.; Dowsett, M. Correlation between cyclooxygenase-2 expression and angiogenesis in human breast cancer. *Clin. Cancer Res.* **2003**, *9*, 2651−2656.
(31) Harris, R. E.; Chlebowski, R. T.; Jackson, R. D.; Frid, D. J.; Ascenseo, J. L.; Anderson, G.; Loar, A.; Rodabough, R. J.; White, E.; McTiernan, A. Breast cancer and nonsteroidal anti-inflammatory drugs: prospective results from the Women's Health Initiative. *Cancer Res.* **2003**, *63*, 6096−6101.
(32) Giovannucci, E.; Egan, K. M.; Hunter, D. J.; Stampfer, M. J.; Colditz, G. A.; Willett, W. C.; Speizer, F. E. Aspirin and the risk of colorectal cancer in women. *N. Engl. J. Med.* **1995**, *333*, 609−614.
(33) Basu, G. D.; Pathangey, L. B.; Tinder, T. L.; Gendler, S. J.; Mukherjee, P. Mechanisms underlying the growth inhibitory effects of the cyclo-oxygenase-2 inhibitor celecoxib in human breast cancer cells. *Breast Cancer Res.* **2005**, *7*, R422−R435.
(34) Minoura, T.; Takata, T.; Sakaguchi, M.; Takada, H.; Yamamura, M.; Hioki, K.; Yamamoto, M. Effect of dietary eicosapentaenoic acid on azoxymethane-induced colon carcinogenesis in rats. *Cancer Res.* **1988**, *48*, 4790−4794.
(35) Bégin, M. E.; Ells, G.; Horrobin, D. F. Polyunsaturated fatty acid-induced cytotoxicity against tumor cells and its relationship to lipid peroxidation. *J. Natl Cancer Inst.* **1988**, *80*, 188−194.
(36) Falconer, J. S.; Ross, J. A.; Fearon, K. C.; Hawkins, R. A.; O'Riordain, M. G.; Carter, D. C. Effect of eicosapentaenoic acid and other fatty acids on the growth *in vitro* of human pancreatic cancer cell lines. *Br. J. Cancer* **1994**, *69*, 826−832.
(37) Palomer, A.; Cabré, F.; Pascual, J.; Campos, J.; Trujillo, M. A.; Entrena, A.; Gallo, M. A.; García, L; Mauleón, D.; Espinosa, A. Identification of novel cyclooxygenase-2 selective inhibitors using pharmacophore models. *J. Med. Chem.* **2002**, *45*, 1402−1411.
(38) Rowlinson, S. W.; Crews, B. C.; Lanzo, C. A.; Marnett, L. J. The binding of arachidonic acid in the cyclooxygenase active site of mouse prostaglandin endoperoxide synthase-2 (COX-2). A putative L-shaped binding conformation utilizing the top channel region. *J. Biol. Chem.* **1999**, *274*, 23305−23310.
(39) Vecchio, A. J.; Simmons, D. M.; Malkowski, M. G. Structural basis of fatty acid substrate binding to cyclooxygenase-2. *J. Biol. Chem.* **2010**, *285*, 22152−22163.
(40) Kiefer, J. R.; Pawlitz, J. L.; Moreland, K. T.; Stegeman, R. A.; Hood, W. F.; Gierse, J. K.; Stevens, A. M.; Goodwin, D. C.; Rowlinson, S. W.; Marnett, L. J.; Stallings, W. C.; Kurumbail, R. G. Structural insights into the stereochemistry of the cyclooxygenase reaction. *Nature* **2000**, *405*, 97−101.
(41) Dong, L.; Vecchio, A. J.; Sharma, N. P.; Jurban, B. J.; Malkowski, M. G.; Smith, W. L. Human cyclooxygenase-2 is a sequence homodimer that functions as a conformational heterodimer. *J. Biol. Chem.* **2011**, *286*, 19035−19046.
(42) Picot, D.; Loll, P. J.; Garavito, R. M. The X-ray crystal structure of the membrane protein prostaglandin H2 synthase-1. *Nature* **1994**, *367*, 243−249.
(43) Kurumbail, R. G.; Stevens, A. M.; Gierse, J. K.; McDonald, J. J.; Stegeman, R. A.; Pak, J. Y.; Gildehaus, D.; Miyashiro, J. M.; Penning, T. D.; Seibert, K.; Isakson, P. C.; Stallings, W. C. Structural basis for

selective inhibition of cyclooxygenase-2 by anti-inflammatory agents. *Nature* **1996**, *384*, 644−648.

(44) Duffy, P. E.; Quinn, S. M.; Roche, H. M.; Evans, P. Synthesis of *trans*-vaccenic acid and *cis*-9-*trans*-11-conjugated linoleic acid. *Tetrahedron* **2006**, *62*, 4838−4843.

(45) Joshi, B. S.; Viswanathan, N.; Gawad, D. H.; Von Philipsborn, W. Piperaceae alkaloids: Part I. Structure of piperstachine; ^{13}C- and ^{1}H-NMR studies. *Helv. Chim. Acta* **1975**, *58*, 1551−1559.

(46) Zhou, J.; Fu, G. C. Palladium-catalyzed Negishi cross-coupling reactions of unactivated alkyl iodides, bromides, chlorides, and tosylates. *J. Am. Chem. Soc.* **2003**, *125*, 12527−12530.

(47) Friesner, R. A.; Murphy, R. B.; Repasky, M. P.; Frye, L. L.; Greenwood, J. R.; Halgren, T. A.; Sanschagrin, P. C.; Mainz, D. T. Extra precision glide: Docking and scoring incorporating a model of hydrophobic enclosure for protein−ligand complexes. *J. Med. Chem.* **2006**, *49*, 6177−6196.